Organic LETTERS

Letter

pubs.acs.org/OrgLett

A Rotary Molecular Motor Gated by Electrical Energy

Chen-Yi Kao,[†] Hsiu-Feng Lu,[‡] Ito Chao,*[,‡] and Jye-Shane Yang*[,†]

[†]Department of Chemistry, National Taiwan University, Taipei, Taiwan 10617

[‡]Institute of Chemistry, Academia Sinica, Taipei, Taiwan 11529

Supporting Information

ABSTRACT: DFT calculations predict that the chiral pentiptycene derivative *E*-**1** possesses distinct rotational potential energy surfaces in the neutral vs the radical anionic (*E*-**1**$^{\bullet-}$) form such that continued electrochemical switching between *E*-**1** and *E*-**1**$^{\bullet-}$ could lead to a directional rotation of the pentiptycene rotor about the exocyclic C−C bond. The time scale of random Brownian rotation is ∼10^6 s for *E*-**1** and ∼170 s for *E*-**1**$^{\bullet-}$ at 150 K, and thus a switching time scale of 0.2 s could readily bias the rotation direction to >99% at 150 K. The synthetic feasibility, line-shape analysis on the VT ^{1}H NMR spectra, and electrochemical redox switching of *E*-**1** are demonstrated.

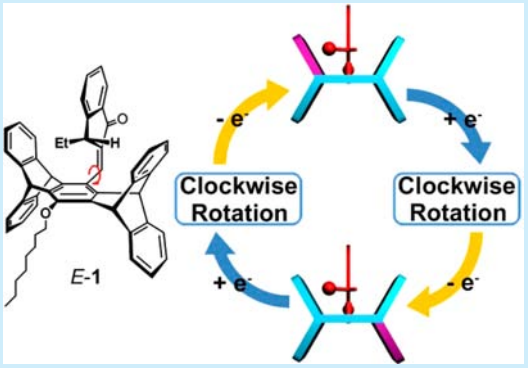

Molecular machines perform designated work at the molecular level. For a (supra-)molecular system to do real work (i.e., a molecular motor), the motional subunit must be able to break the detailed balance of Brownian motions, namely, to undergo biased or directional motion in response to the input of energies.[1,2] While naturally occurring molecular motors such as ATP synthase, kinesin, and myosin adopt chemical fuels,[3] artificial counterparts could be driven by other types of energy such as light and electrical energy.[1,2] To date, only a few prototypes of rotary molecular motors have been reported,[4] including Feringa's light-driven tetrasubstituted alkenes[5] and chemical-driven lactone system,[6] Leigh's macrocycle system powered by both light and chemicals,[7] Lehn's light-driven diaryl-*N*-alkyl imines,[8] and Rapenne−Joachim−Hla's ruthenium complex powered by electrical energy.[9] For those fueled by electrical energy,[9,10] the operation is on a single molecule with an STM tip positioned over the molecule or at a specific site of the molecule for the injection of electrons at low temperatures (<10 K). The rotation is based on energy transfer from the tunneling electron to the molecule that leads to an electronic excited state, in analogy to the effect of photoexcitation. We report herein a new rotary molecular motor (*E*-**1**, Figure 1a) that uses electrical energy to trigger redox reactions and thus bias the Brownian rotation. Such an operation mechanism differs from that in the STM-driven systems and allows one to carry on an ensemble of molecules at relatively high temperatures (∼180 K).

The chiral molecular motor *E*-**1** was designed on the basis of the achiral precursor *E*-**2** (Figure 1b), which was investigated as a molecular brake on the basis of interconvertable *E* and *Z* isomers; the photochemical switching of *E*-**2** → *Z*-**2** results in a decrease of the rotation rate by 500-fold for the pentiptycene rotor about the external C−C bond, mimicking brake performance.[11] The reverse switching of *Z*-**2** → *E*-**2** that recovers the brake-off state was effectively achieved by electrochemical redox-gating via the radical anion intermediates that thermodynamically favor the *E* isomer (i.e., *Z*-**2** → *Z*-**2**$^{\bullet-}$ →*E*-**2**$^{\bullet-}$ → *E*-**2**). The moderate rotation rate at room temperature (∼2 × 10^4 s^{-1}), high electrochemical stability, and tunable structure for *E*-**2** provide a unique opportunity toward a Brownian molecular motor.[1,12] We reasoned that enantioselective substitution at the indanone methylene group could have two effects: (1) creating a chirality center and thus a ratchet rotational potential energy surface (RPES); (2) increasing the torsion barrier and thus minimizing the random Brownian rotation at ambient temperatures. Provided that the RPES for the neutral and the anion radical states of *E*-**1** differ in a way that biased rotation can be achieved through electrochemical switching between *E*-**1** and *E*-**1**$^{\bullet-}$, directional rotation of *E*-**1** gated by electrical energy would be achieved via the "Pulsating Ratchet" mechanism.[1]

Scheme 1 shows the synthesis of *E*-**1**. The Horner−Wadsworth−Emmons reaction between propiophenone and triethyl phosphonoacetate led to the cinnamic acid ester **3**. Asymmetrical conjugated reduction of **3** with CuCl and PMHS (polymethylhydrosiloxane) in the presence of the (*S*)-*p*-tol-BINAP ligand[13] followed by base-catalyzed hydrolysis of the ester group produced the chiral acid **4** with an *S* configuration for the chirality center. Cyclization of **4** promoted by PPA (polyphosphoric acid) led to the optically active indanone **5**[14] with a 90% ee value. The target system *E*-**1** was obtained through a base-catalyzed aldol condensation reaction between **5** and the previously reported pentiptycene building block **6**[15] under microwave irradiation. The basic conditions for aldol condensation do not racemize the chirality center in **5** but somewhat decrease the ee value from 90% to 81% in a "blank" **6**-free

Received: October 6, 2014
Published: November 13, 2014

 © 2014 American Chemical Society dx.doi.org/10.1021/ol502946v | *Org. Lett.* 2014, 16, 6100−6103

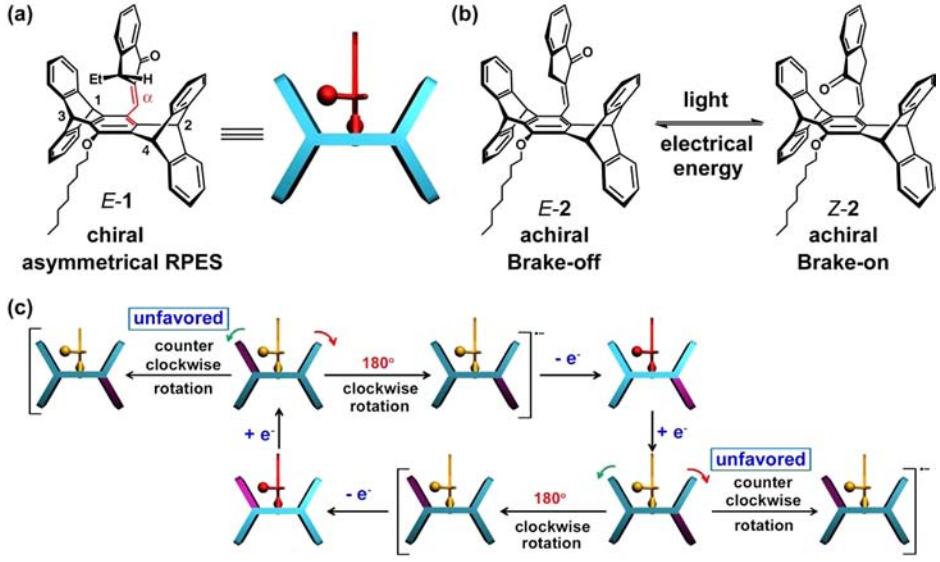

Figure 1. (a) Design of a chiral and electrical energy-gated molecular motor *E*-**1** from (b) an achiral molecular brake precursor *E*-**2** that is operated by light and electrical energy and (c) schematic drawing of the operation concept for the directional rotation of *E*-**1**, in which switching from the rotation-inhibited neutral form to the radical anionic form allows a biased clockwise rotation of the pentiptycene rotor. For the clarity of the rotational motion, one of the pentiptycene blades is labeled with a different color. The red C═C−C═C bond in (a) defines the twist angle α for discussion in the text.

Scheme 1. Synthesis of *E*-1

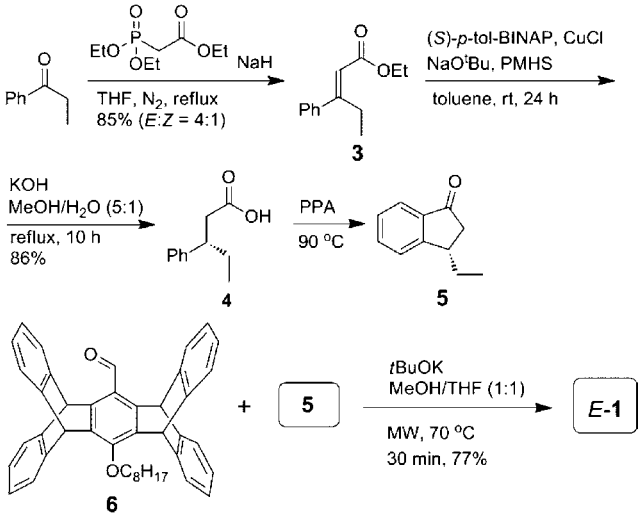

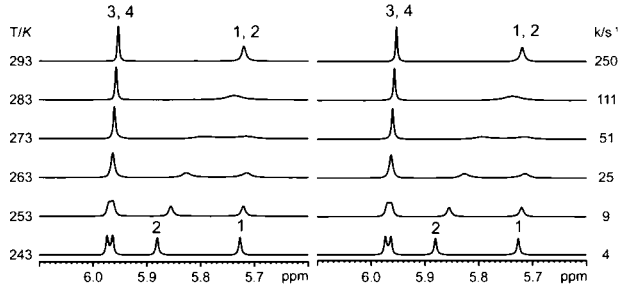

Figure 2. Variable-temperature ^{1}H NMR (left) and simulated (right) spectra of *E*-**1** in DMF-d_7 at the region of bridgehead protons. Values of temperature (T in K) and the interconversion rate (k in s^{-1}) are also given for each trace.

experiment. Assuming that the same ee value of 81% is retained in the product *E*-**1**, the specific rotation of *E*-**1** in $CHCl_3$ at 23 °C ($[\alpha]^{23}_D$) could be estimated to be +10.9°. The corresponding CD spectrum is shown in Figure S1. Chiral resolution of *E*-**1** was not performed.

The rotational kinetics of *E*-**1** have been investigated by variable temperature (VT) ^{1}H NMR spectroscopy. Because of the presence of a chirality center in the indanone moiety, the four bridgehead proton signals of the pentiptycene rotor have different chemical shifts when the rotation is slower than the NMR time scale. This is indeed observed for *E*-**1** in DMF-d_7 at 243 K (Figure 2). The peak assignment was accomplished with 2D NMR spectra, including NOESY, ROESY, COSY, HMBC, and HSQC (Figures S2−S6). Line-shape analysis on the bridgehead proton signals provided the information on rotation rates at each temperature, and the activation parameters derived from Arrhenius and Eyring plots (Figures S7 and S8) are listed in Table S1. Compared to *E*-**2**, *E*-**1** displays a larger activation barrier (E_a = 11.9 vs 8.3 kcal mol^{-1}), preexponential value (log A = 11.3 vs 10.6), and enthalpy of activation ($\Delta H^{\ddagger}$ = 11.4 vs 7.8 kcal mol^{-1}) but less negative entropy of activation ($\Delta S^{\ddagger}$ = −8.7 vs −12.0 cal mol^{-1} K^{-1}). Consequently, the replacement of a hydrogen in the indanone methylene moiety with an ethyl group raises the free energy of activation ($\Delta G^{\ddagger}$) by ∼2.5 kcal mol^{-1} at 298 K. On the basis of the activation parameters, the rotation rate for *E*-**1** would be lower than 0.02 s^{-1} at 200 K.

The RPES for *E*-**1** was constructed by DFT calculations at the B3LYP/6-31G(d) level (Figure 3a). To simplify the calculation, the octyl group was replaced with a methyl group. The fully optimized local minimum shows a twist angle α of −65.8° that is defined by the pentiptycene−methinylindanone C═C−C═C dihedral angle (Figure 1a). By looking straight down the external C−C bond with the pentiptycene rotor in the front, clockwise rotation of the rotor by ∼96° reaches the transition state TS_C (α = −161.8°), but the transition state TS_{CC} (α = 16.6°) for counterclockwise rotation is reached at a rotation of ∼82°, revealing an asymmetric RPES. Gibbs free energy correction was applied to the fully optimized local maximum and minimum of the RPES at the BMK/6-311+G(d,p)//B3LYP/6-31G(d) level (see Supporting Information). At 298 K the transition states are ∼13.5 kcal mol^{-1} higher in free energy than the optimized

dx.doi.org/10.1021/ol502946v | *Org. Lett.* 2014, 16, 6100−6103

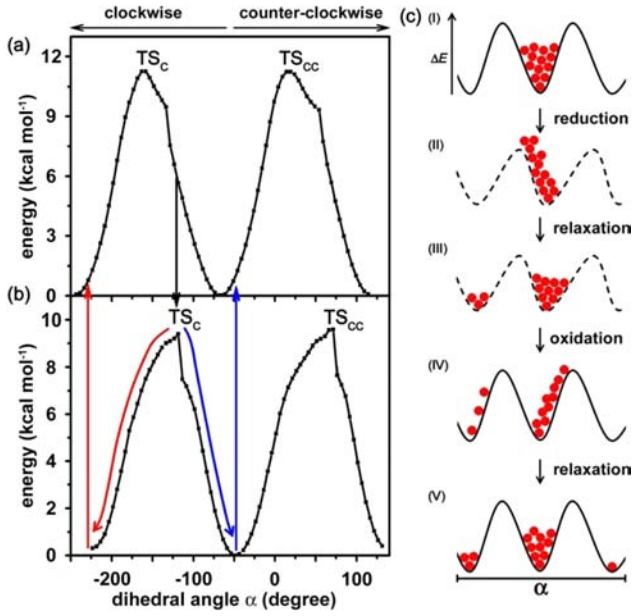

Figure 3. DFT-derived rotational potential energy surface (RPES) for the pentiptycene rotor in (a) *E*-**1** and (b) *E*-**1**$^{\bullet-}$ about the external C−C bond in both clockwise and counterclockwise directions (see Figure 1c for definition), and (c) schematic representation of the concept of directional rotation triggered by electrochemical switching between *E*-**1** and *E*-**1**$^{\bullet-}$.

ground state, which is in excellent agreement with the experimental value of 13.9 kcal mol^{-1} for the activation energy of rotation. The transition states TS_C and TS_{CC} encounter not only the steric repulsion between the protons on the pentiptycene bridgehead and on the methinyl carbons but also a distorted C−C═C bond angle for the methinyl carbon from 128° in the ground state to ∼143° in the transition states (Table S2).

The RPES for *E*-**1**$^{\bullet-}$ (Figure 3b) was also constructed by DFT calculations at the same level of theory as that for *E*-**1**. The ground state possesses a smaller twist angle α of −48.7° as compared to the neutral form (−65.8°). The TS_C (α = −116.3°) is reached with a clockwise rotation of the pentiptycene rotor by ∼67°, and the TS_{CC} (α = 70.7°) is formed with a counterclockwise rotation by ∼119°, again corresponding to an asymmetric RPES. The calculated $\Delta G^{\ddagger}$ is 10.8 kcal mol^{-1} for *E*-**1**$^{\bullet-}$ at 298 K, which is 2.7 kcal mol^{-1} lower than that for *E*-**1**. The difference in RPES for *E*-**1**$^{\bullet-}$ vs *E*-**1** could be understood by the fact that adding an electron to the π^* orbital of a conjugated system reduces the bond order of a double bond and increases that of a single bond, as indicated by the lengthened exocyclic C═C bond (1.38 vs 1.34 Å) and shortened exocyclic C−C bond (1.45 vs 1.48 Å). The increased bond order for the exocyclic C−C bond accounts for the decrease of α in the ground state. An increase of structural planarity for π-conjugated systems upon oxidation or reduction has also been experimentally demonstrated.[16] The decreased bond order for the exocyclic C═C bond makes the methinylindanone moiety less rigid and thus shifts the positions of the transition states and reduces the rotation barrier. It was also predicted that isomerization from *E*-**1**$^{\bullet-}$ to *Z*-**1**$^{\bullet-}$ is energetically unfavorable, because the latter is less stable than the former by 0.84 kcal mol^{-1} (Figure S9). This value is likely underestimated according to the results of HPLC analysis on *E*-**1** after electrochemical treatment (*vide infra*).

The differences in RPES for *E*-**1** vs *E*-**1**$^{\bullet-}$ provide an opportunity toward directional rotary operation gated by electrical energy. When the temperature is lowered so that Brownian rotation is very slow, a switching from *E*-**1** to *E*-**1**$^{\bullet-}$ could lead to a position near the TSc of *E*-**1**$^{\bullet-}$ (black vertical arrow in Figure 3a), which would relax to the ground state of *E*-**1**$^{\bullet-}$ either through clockwise (red curved arrow in Figure 3b) or counterclockwise (blue curved arrow in Figure 3b) rotation. A reverse switching of *E*-**1**$^{\bullet-}$ back to *E*-**1** finishes a clockwise rotation of 180° for the clockwise relaxed portion (red vertical arrow in Figure 3b), but it recovers the original status of *E*-**1** for the counterclockwise relaxed portion (blue vertical arrow in Figure 3b). Figure 3c depicts such a pulsating ratchet mechanism, in which the solid and dashed curves represent the RPES of *E*-**1** and *E*-**1**$^{\bullet-}$, respectively, and the red dots represent the position of the rotors along the RPES. At low temperatures, a Brownian rocking motion between the transition states TS_C and TS_{CC} is expected to dominate the torsions (RPES I). When electrical energy is applied and *E*-**1**$^{\bullet-}$ is formed, some molecules would end up near the TS_C of *E*-**1**$^{\bullet-}$ (RPES II) and relax clockwise (RPES III). Oxidation of *E*-**1**$^{\bullet-}$ back to *E*-**1** (RPES IV) followed by relaxation led to a net clockwise rotation of 180° (RPES V). Continued performance of double potential steps that repeat the switching cycle of *E*-**1** → *E*-**1**$^{\bullet-}$ → *E*-**1** would continuously drive the 180° clockwise rotation for the pentiptycene rotor as long as the electrochemical switching is faster than the random Brownian rotation, leading to directional or biased clockwise rotation of the system. A schematic drawing of the electrical energy-biased rotation is depicted in Figure 1c. It should be noted that at the moment of electron transfer, either *E*-**1** → *E*-**1**$^{\bullet-}$ or *E*-**1**$^{\bullet-}$ → *E*-**1**, the unrelaxed product is 3−6 kcal mol^{-1} higher than the relaxed form (Figure S10). Nevertheless, this will not affect the pulsating ratchet gating of the rotation.

In principle, the electrochemical switching time scale must be shorter than the time scale for random Brownian rotation to bias the rotation direction, and as the time scale difference increases, so does the rotation directionality. At 298 K, each Brownian rotation takes 3.0×10^{-3} and 1.4×10^{-5} s for *E*-**1** and *E*-**1**$^{\bullet-}$, respectively. This indicates that the potential pulse time for the double potential step switching must be shorter than 10 μs to bias the rotation direction at 298 K. However, the Brownian rotation rate could be largely reduced at lower temperatures. For example, according to the activation parameters, the Brownian rotation time scale becomes ∼900 s for *E*-**1** and ∼0.73 s for *E*-**1**$^{\bullet-}$ at 180 K and is ∼10^6 s for *E*-**1** and ∼170 s for *E*-**1**$^{\bullet-}$ at 150 K. Therefore, the use of potential pulse times of 0.1 s would bias the rotation direction to ∼70% at 180 K and to >99% at 150 K.[17] Such an operation temperature is considerably higher than that (<10 K) for STM-based single molecule systems.[9,10]

The robustness of electrochemical switching between *E*-**1** and *E*-**1**$^{\bullet-}$ is evidenced by the persistent cyclic voltammograms (Figure 4a) and by the stable chronocoulometric charge−time curves (Figure 4b). The initial and final potentials were 1.40 and −1.70 V relative to the ferrocene/ferrocenium redox couple (Fc/Fc$^+$), respectively. The pulse time for chronocoulometry was 0.2 s, but a pulse time as short as 100 μs was also achievable (Figure S11). The stability of *E*-**1**$^{\bullet-}$ relative to the isomer *Z*-**1**$^{\bullet-}$ was also investigated by HPLC analysis on the solution after 100 and 200 cycles of switching (Figure 4c). An authentic sample of *Z*-**1** was prepared by the irradiation of *E*-**1** in DCM at 306 nm (see Supporting Information). The results showed that the *E*/*Z* ratio is 99:1 and 97:3 after 100 and 200 cycles of switching, respectively. The latter is similar to that observed for the achiral

dx.doi.org/10.1021/ol502946v | *Org. Lett.* 2014, 16, 6100−6103

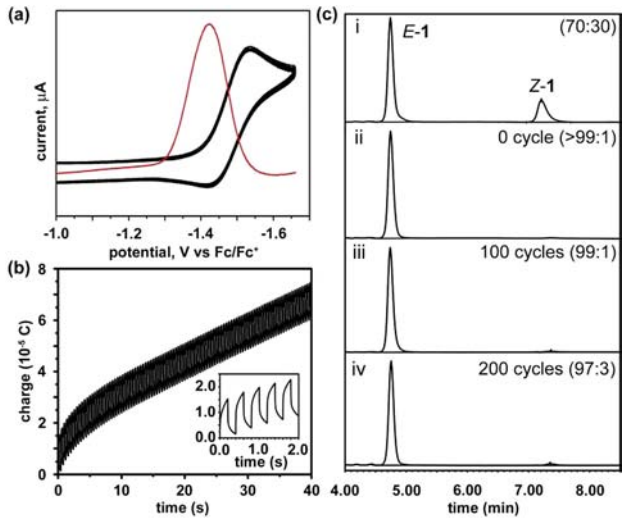

Figure 4. (a) Differential pulse voltammogram (red) and overlay plot of 5 cyclic voltammograms (black) of *E*-**1** in DCM (0.55 mM) with 0.1 M Bu_4NPF_6 at a scan rate of 100 mV s^{-1} and (b) chronocoulometric diagram of *E*-**1** with 100 cycles of alternating switching of applied electric potential at −1.7 and 1.4 V (vs Fc/Fc^+) for 0.2 s, and the first 5 cycles are shown in the inset figure; (c) HPLC trace of (i) *E*-**1** and *Z*-**1** mixture, (ii) *E*-**1** only, and the solution of *E*-**1** after (iii) 100 and (iv) 200 cycles of chronocoulometric measurements (pulse time is 0.2 s).

precursor *E*-**2** (96:4).[11] All these data secure the electrical energy-gated operation of molecular motor *E*-**1**.

In summary, the distinct rotational potential energy surfaces for *E*-**1** in the neutral vs the radical anionic forms and the reliable electrochemical switching between the two forms pave a path toward a new Brownian motor that is gated by electrical energy. The pulsating ratchet mechanism renders this system to be operable at much higher temperatures than the previously reported electrical energy-gated molecular motors.[9,10]

■ ASSOCIATED CONTENT

Supporting Information

Experimental methods, synthetic details, 1D and 2D NMR spectra, Arrhenius and Eyring plots, activation parameters for the rotation, and DFT-calculated structural parameters. The material is available free of charge via the Internet at http://pubs.acs.org.

■ AUTHOR INFORMATION

Corresponding Authors

*E-mail: jsyang@ntu.edu.tw.
*E-mail: ichao@chem.sinica.edu.tw.

Notes

The authors declare no competing financial interest.

■ ACKNOWLEDGMENTS

We thank the Ministry of Science and Technology of Taiwan and National Taiwan University for financial support. The authors thank Prof. Ying-Chih Lin and Ms. Shou-Ling Huang (NTU) for the support of VT NMR measurements.

■ REFERENCES

(1) Kay, E. R.; Leigh, D. A.; Zerbetto, F. *Angew. Chem., Int. Ed.* **2007**, *46*, 72−191.
(2) (a) Kottas, G. S.; Clarke, L. I.; Horinek, D.; Michl, J. *Chem. Rev.* **2005**, *105*, 1281−1376. (b) Coskun, A.; Banaszak, M.; Astumian, R. D.; Stoddart, J. F.; Grzybowski, B. A. *Chem. Soc. Rev.* **2012**, *41*, 19−30.
(3) Kinbara, K.; Aida, T. *Chem. Rev.* **2005**, *105*, 1377−1400.
(4) Kelly's triptycene-helicene system provides an early example of directional rotation, but it is not a full 360° rotation; see: Kelly, T. R.; De Silva, H.; Silva, R. A. *Nature* **1999**, *401*, 150−152.
(5) (a) Koumura, N.; Zijlstra, R. W. J.; van Delden, R. A.; Harada, N.; Feringa, B. L. *Nature* **1999**, *401*, 152−155. (b) Feringa, B. L. *J. Org. Chem.* **2007**, *72*, 6635−6652.
(6) Fletcher, S. P.; Dumur, F.; Pollard, M. M.; Feringa, B. L. *Science* **2005**, *310*, 80−82.
(7) Leigh, D. A.; Wong, J. K. Y.; Dehez, F.; Zerbetto, F. *Nature* **2003**, *424*, 174−179.
(8) Greb, L.; Lehn, J.-M. *J. Am. Chem. Soc.* **2014**, *136*, 13114−13117.
(9) Perera, U. G. E.; Ample, F.; Kersell, H.; Zhang, Y.; Vives, G.; Echeverria, J.; Grisolia, M.; Rapenne, G.; Joachim, C.; Hla, S. W. *Nat. Nanotechnol.* **2013**, *8*, 46−51.
(10) Kudernac, T.; Ruangsupapichat, N.; Parschau, M.; Macia, B.; Katsonis, N.; Harutyunyan, S. R.; Ernst, K.-H.; Feringa, B. L. *Nature* **2011**, *479*, 208−211.
(11) Chen, Y.-C.; Sun, W.-T.; Lu, H.-F.; Chao, I.; Huang, G.-J.; Lin, Y.-C.; Huang, S.-L.; Huang, H.-H.; Lin, Y.-D.; Yang, J.-S. *Chem.—Eur. J.* **2011**, *17*, 1193−1200.
(12) Astumian, R. D. *Science* **1997**, *276*, 917−922.
(13) Appella, D. H.; Moritani, Y.; Shintani, R.; Ferreira, E. M.; Buchwald, S. L. *J. Am. Chem. Soc.* **1999**, *121*, 9473−9474.
(14) Stephan, E.; Rocher, R.; Aubouet, J.; Pourcelot, G.; Cresson, P. *Tetrahedron: Asymmetry* **1994**, *5*, 41−44.
(15) Yang, J.-S.; Ko, C.-W. *J. Org. Chem.* **2006**, *71*, 844−847.
(16) Fujitsuka, M.; Tojo, S.; Yang, J.-S.; Majima, T. *Chem. Phys.* **2013**, *419*, 118−123.
(17) The rotation directionality (r.d.) was calculated according to the equation: r.d. = $(t_B - 2t_{ps})/t_B$, where t_B is the time for a 180° Brownian rotation in *E*-$\mathbf{1}^{\bullet-}$ and $2t_{ps}$ denotes the time for each redox switching cycle *E*-**1** → *E*-$\mathbf{1}^{\bullet-}$ → *E*-**1** that consists of double potential switching (t_{ps}).